

The study of lepton EDM in CP violating BLMSSM

Shu-Min Zhao^{1*}, Tai-Fu Feng^{1†}, Xi-Jie Zhan¹, Hai-Bin Zhang^{1,2}, Ben Yan¹

¹ *Department of Physics, Hebei University, Baoding 071002, China*

² *Department of Physics, Dalian University of Technology, Dalian 116024, China*

(Dated: October 29, 2018)

Abstract

In the supersymmetric model with local gauged baryon and lepton numbers(BLMSSM), the CP violating effects are considered to study the lepton electric dipole moment(EDM). The CP violating phases in BLMSSM are more than those in the standard model(SM) and can give large contributions. The analysis of the EDMs for the leptons e, μ, τ is shown in this work. It is in favour of exploring the source of CP violation and probing the physics beyond SM.

PACS numbers: 13.40.Em, 12.60.-i

Keywords: CP violating, electric dipole moment, lepton

* zhaosm@hbu.edu.cn

† fengtf@hbu.edu.cn

I. INTRODUCTION

The theoretical predictions for EDMs of leptons and neutron are very small in SM. The estimated SM value for the electron EDM is about $|d_e| \simeq 10^{-38} e.cm$ [1], which is too small to be detected by the current experiments. The ACME Collaboration[2] report the new result of electron EDM $d_e = (-2.1 \pm 3.7_{stat} \pm 2.5_{syst}) \times 10^{-29} e.cm$. The upper bound of electron EDM is $|d_e| < 8.7 \times 10^{-29} e.cm$ at the 90% confidence level. Therefore, if large EDM of electron is probed, one can ensure it is the signal of new physics beyond SM. $|d_\mu| < 1.9 \times 10^{-19} e.cm$ and $|d_\tau| < 10^{-17} e.cm$ are the EDM upper bounds of μ and τ respectively[3]. The minimal supersymmetric extension of SM (MSSM) [4] is very attractive and physicists have studied it for a long time. In MSSM, there are a lot of CP violating phases and they can give large contributions to the EDMs of leptons and neutron.

In MSSM, when the CP violating phases are of normal size and the SUSY particles are at TeV scale, big EDMs of elementary particles are obtained, and they can exceed the current experiment limits. Three approaches are used to resolve this problem. 1. make the CP violating phases small, i.e. $O(10^{-2})$. That is the so called tuning. 2. use mass suppression through making SUSY particles heavy (several TeV). 3. there is cancellation mechanism among the different components. For lepton EDM and neutron EDM, the main parts of chargino and the neutralino contributions are cancelled[5].

BLMSSM is the minimal supersymmetric extension of the SM with local gauged B and L[6]. Therefore, it can explain both the asymmetry of matter-antimatter in the universe and the data from neutrino oscillation experiment. We consider that BLMSSM is a favorite model beyond MSSM. Extending SM, the authors study the model with B and L as spontaneously broken gauge symmetries around TeV scale[7]. The lightest CP-even Higgs mass and the decays $h^0 \rightarrow \gamma\gamma$, $h^0 \rightarrow ZZ(WW)$ are also studied in this model[8]. In our previous works[9, 10], we study the neutron EDM and $B^0 - \bar{B}^0$ mixing in CP violating BLMSSM.

Research the MDMs [11] and EDMs[12, 13] of leptons are the effective ways to probe new physics beyond the SM. In MSSM, the one-loop contributions to lepton MDM and EDM are well studied, and some two loop corrections are also investigated. In the two Higgs doublet models with CP violation, the authors obtain the one-loop and Barr-Zee type two-loop contributions to fermionic EDMs. A model-independent study of d_e in the SM is carried out[14]. They take into account the right-handed neutrinos, the neutrino see-saw

mechanism and the framework of minimal flavor violation. Their results show that when neutrinos are Majorana particles, d_e can reach its experiment upper bound.

After this introduction, in section 2 we briefly introduce the main ingredients of the BLMSSM. The one-loop corrections to the lepton EDM are collected in section 3. Section 4 is devoted to the numerical analysis for the dependence of lepton EDM on the BLMSSM parameters. We show our discussion and conclusion in section 5.

II. THE BLMSSM

The local gauge group of BLMSSM[6] is $SU(3)_C \otimes SU(2)_L \otimes U(1)_Y \otimes U(1)_B \otimes U(1)_L$, where the exotic leptons are introduced to cancel L anomaly. Similarly, they introduce the exotic quarks to cancel the B anomaly. In this work, the quarks, exotic quarks and exotic leptons have none one-loop contribution to lepton EDM, so we do not introduce them in detail. The Higgs mechanism is of solid foundation, because of the detection of the lightest CP even Higgs h^0 at LHC[15]. The Higgs superfields are used to break lepton number spontaneously, and they need nonzero vacuum expectation values (VEVs).

The superpotential of BLMSSM is shown as

$$\mathcal{W}_{BLMSSM} = \mathcal{W}_{MSSM} + \mathcal{W}_B + \mathcal{W}_L + \mathcal{W}_X . \quad (1)$$

Here, \mathcal{W}_{MSSM} represents the superpotential of the MSSM. The concrete forms of \mathcal{W}_B , \mathcal{W}_L and \mathcal{W}_X are shown in the work[8]. \mathcal{W}_L includes the needed new term $\mathcal{W}_L(n)$, which is collected here

$$\mathcal{W}_L(n) = Y_\nu \hat{L} \hat{H}_u \hat{N}^c + \lambda_{N^c} \hat{N}^c \hat{N}^c \hat{\varphi}_L + \mu_L \hat{\Phi}_L \hat{\varphi}_L . \quad (2)$$

In BLMSSM, the complete soft breaking terms are very complex[8, 9], and only the terms relating with lepton are necessary for our study

$$\begin{aligned} \mathcal{L}_{soft}(L) = & -m_{\tilde{N}^c}^2 \tilde{N}^{c*} \tilde{N}^c - m_{\Phi_L}^2 \Phi_L^* \Phi_L - m_{\varphi_L}^2 \varphi_L^* \varphi_L - (M_L \lambda_L \lambda_L + h.c.) \\ & + (A_N Y_\nu \tilde{L} H_u \tilde{N}^c + A_{N^c} \lambda_{N^c} \tilde{N}^c \tilde{N}^c \varphi_L + B_L \mu_L \Phi_L \varphi_L + h.c.) . \end{aligned} \quad (3)$$

In order to break the local gauge symmetry $SU(2)_L \otimes U(1)_Y \otimes U(1)_B \otimes U(1)_L$ down to the electromagnetic symmetry $U(1)_e$, the $SU(2)_L$ doublets H_u and H_d should obtain nonzero

VEVs v_u and v_d . While the $SU(2)_L$ singlets Φ_L and φ_L should obtain nonzero VEVs v_L and \bar{v}_L respectively. The needed Higgs fields and Higgs superfields are defined as

$$\begin{aligned} H_u &= \begin{pmatrix} H_u^+ \\ \frac{1}{\sqrt{2}}(v_u + H_u^0 + iP_u^0) \end{pmatrix}, & H_d &= \begin{pmatrix} \frac{1}{\sqrt{2}}(v_d + H_d^0 + iP_d^0) \\ H_d^- \end{pmatrix}, \\ \Phi_L &= \frac{1}{\sqrt{2}}(v_L + \Phi_L^0 + iP_L^0), & \varphi_L &= \frac{1}{\sqrt{2}}(\bar{v}_L + \varphi_L^0 + i\bar{P}_L^0). \end{aligned} \quad (4)$$

The detailed discussion of Higgs mass matrices can be found in Ref.[8]. The super field \hat{N}^c in BLMSSM leads to that the neutrinos and sneutrinos are doubled as those in MSSM. Through the see-saw mechanism, light neutrinos obtain tiny masses.

In BLMSSM, there are 10 neutralinos: 4 MSSM neutralinos, 3 baryon neutralinos and 3 lepton neutralinos. The MSSM neutralinos, baryon neutralinos and lepton neutralinos do not mix with each other. Baryon neutralinos have zero contribution to the lepton EDM at one-loop level. While, lepton neutralinos can give contributions to lepton EDM through lepton-slepton-lepton neutralino coupling. The three lepton neutralinos are made up of λ_L (the superpartners of the new lepton boson) and $\psi_{\Phi_L}, \psi_{\varphi_L}$ (the superpartners of the $SU(2)_L$ singlets Φ_L, φ_L). Here, we show the mass term of lepton neutralinos.

$$\mathcal{L}_{\chi_L^0} = \frac{1}{2}(i\lambda_L, \psi_{\Phi_L}, \psi_{\varphi_L}) \begin{pmatrix} 2M_L & 2v_L g_L & -2\bar{v}_L g_L \\ 2v_L g_L & 0 & -\mu_L \\ -2\bar{v}_L g_L & -\mu_L & 0 \end{pmatrix} \begin{pmatrix} i\lambda_L \\ \psi_{\Phi_L} \\ \psi_{\varphi_L} \end{pmatrix} + h.c. \quad (5)$$

Three lepton neutralino masses are obtained from diagonalizing the mass mixing matrix in Eq.(5) by Z_{N_L} .

Though in BLMSSM there are six sleptons, their mass squared matrix is different from that in MSSM, because of the contributions from Eqs.(2,3). We deduce the corrected mass squared matrix of slepton, and the matrix $Z_{\tilde{L}}$ is used to diagonalize it

$$\begin{pmatrix} (\mathcal{M}_L^2)_{LL} & (\mathcal{M}_L^2)_{LR} \\ (\mathcal{M}_L^2)_{LR}^\dagger & (\mathcal{M}_L^2)_{RR} \end{pmatrix}. \quad (6)$$

$(\mathcal{M}_L^2)_{LL}$, $(\mathcal{M}_L^2)_{LR}$ and $(\mathcal{M}_L^2)_{RR}$ are shown as

$$\begin{aligned} (\mathcal{M}_L^2)_{LL} &= \frac{(g_1^2 - g_2^2)(v_d^2 - v_u^2)}{8}\delta_{IJ} + g_L^2(\bar{v}_L^2 - v_L^2)\delta_{IJ} + m_{\tilde{l}^c}^2\delta_{IJ} + (m_{\tilde{L}}^2)_{IJ}, \\ (\mathcal{M}_L^2)_{LR} &= \frac{\mu^* v_u}{\sqrt{2}}(Y_l)_{IJ} - \frac{v_u}{\sqrt{2}}(A'_l)_{IJ} + \frac{v_d}{\sqrt{2}}(A_l)_{IJ}, \\ (\mathcal{M}_L^2)_{RR} &= \frac{g_1^2(v_u^2 - v_d^2)}{4}\delta_{IJ} - g_L^2(\bar{v}_L^2 - v_L^2)\delta_{IJ} + m_{\tilde{l}^c}^2\delta_{IJ} + (m_{\tilde{R}}^2)_{IJ}. \end{aligned} \quad (7)$$

The super field \hat{N}^c is introduced in BLMSSM, so the sneutrino mass matrix and the sneutrino mass squared matrix are both 6×6 and more complicated than those in MSSM. In the left-handed basis (ν, N^c) , we deduce the mass matrix of neutrino after symmetry breaking

$$-\mathcal{L}_{mass}^\nu = (\bar{\nu}_R^I, \bar{N}_R^{cI}) \begin{pmatrix} 0 & \frac{v_u}{\sqrt{2}}(Y_\nu)_{IJ} \\ \frac{v_u}{\sqrt{2}}(Y_\nu^T)_{IJ} & \frac{\bar{v}_L}{\sqrt{2}}(\lambda_{N^c})_{IJ} \end{pmatrix} \begin{pmatrix} \nu_L^J \\ N_L^{cJ} \end{pmatrix} + h.c. \quad (8)$$

With the unitary transformations

$$\begin{pmatrix} \nu_{1L}^I \\ \nu_{2L}^I \end{pmatrix} = U_{\nu^{IJ}}^\dagger \begin{pmatrix} \nu_L^J \\ N_L^{cJ} \end{pmatrix}, \quad \begin{pmatrix} \nu_{1R}^I \\ \nu_{2R}^I \end{pmatrix} = W_{\nu^{IJ}}^\dagger \begin{pmatrix} \nu_R^J \\ N_R^{cJ} \end{pmatrix}, \quad (9)$$

the mass matrix of neutrino is diagonalized as

$$W_{\nu^{IJ}}^\dagger \begin{pmatrix} 0 & \frac{v_u}{\sqrt{2}}(Y_\nu)_{IJ} \\ \frac{v_u}{\sqrt{2}}(Y_\nu^T)_{IJ} & \frac{\bar{v}_L}{\sqrt{2}}(\lambda_{N^c})_{IJ} \end{pmatrix} U_{\nu^{IJ}} = \text{diag}(m_{\nu_1^I}, m_{\nu_2^I}). \quad (10)$$

The trilinear sneutrino-Higgs-sneutrino coupling $A_{N^c} \lambda_{N^c} \tilde{N}^c \tilde{N}^c \varphi_L$ in the soft breaking terms $\mathcal{L}_{soft}(L)$ leads to large sneutrino masses. The VEV of φ_L is $\frac{1}{\sqrt{2}}\bar{v}_L$, and the contribution from this term to sneutrino masses is at the order of $A_{N^c} \lambda_{N^c} \bar{v}_L$. The super potential of BLMSSM includes the new term $\mathcal{W}_L(n)$. Then two functions and the scalar supersymmetric potential are shown here

$$\begin{aligned} F_i &= \frac{\partial W}{\partial A_i}, & D^a &= g A_i^* T_{ij}^a A_j, \\ V &= \frac{1}{2} D^a D^a + F_i^* F_i, \end{aligned} \quad (11)$$

where A_i represent the scalar fields. The first term $Y_\nu \hat{L} \hat{H}_u \hat{N}^c$ in $\mathcal{W}_L(n)$ is suppressed by Y_ν . Using the formula Eq.(2), the second term $\lambda_{N^c} \hat{N}^c \hat{N}^c \hat{\varphi}_L$ in $\mathcal{W}_L(n)$ can give important contributions to large sneutrino masses through nonzero VEV of Higgs superfield φ_L . This type correction is at the order of $\lambda_{N^c}^* \lambda_{N^c} \bar{v}_L^2$. The orders of both dominant contributions respectively are $A_{N^c} \lambda_{N^c} \bar{v}_L$ and $\lambda_{N^c}^* \lambda_{N^c} \bar{v}_L^2$, that are much larger than the product of neutrino Yukawa and SUSY scale. The mass squared matrix of the sneutrino is obtained from the superpotential and the soft breaking terms from Eqs.(2)(3),

$$-\mathcal{L}_{\tilde{n}}^{mass} = \tilde{n}^\dagger \cdot \mathcal{M}_{\tilde{n}}^2 \cdot \tilde{n}, \quad (12)$$

with $\tilde{n}^T = (\tilde{\nu}, \tilde{N}^{c*})$. The sneutrinos are enlarged by the superfield \hat{N}^c and the mass squared matrix of sneutrino reads as

$$\begin{aligned}\mathcal{M}_{\tilde{n}}^2(\tilde{\nu}_I^* \tilde{\nu}_J) &= \frac{g_1^2 + g_2^2}{8}(v_d^2 - v_u^2)\delta_{IJ} + g_L^2(\bar{v}_L^2 - v_L^2)\delta_{IJ} + \frac{v_u^2}{2}(Y_\nu^\dagger Y_\nu)_{IJ} + (m_{\tilde{L}}^2)_{IJ}, \\ \mathcal{M}_{\tilde{n}}^2(\tilde{N}_I^{c*} \tilde{N}_J^c) &= -g_L^2(\bar{v}_L^2 - v_L^2)\delta_{IJ} + \frac{v_u^2}{2}(Y_\nu^\dagger Y_\nu)_{IJ} + 2\bar{v}_L^2(\lambda_{N^c}^\dagger \lambda_{N^c})_{IJ} \\ &\quad + (m_{\tilde{N}^c}^2)_{IJ} + \mu_L \frac{v_L}{\sqrt{2}}(\lambda_{N^c})_{IJ} - \frac{\bar{v}_L}{\sqrt{2}}(A_{N^c})_{IJ}(\lambda_{N^c})_{IJ}, \\ \mathcal{M}_{\tilde{n}}^2(\tilde{\nu}_I \tilde{N}_J^c) &= \mu^* \frac{v_d}{\sqrt{2}}(Y_\nu)_{IJ} - v_u \bar{v}_L (Y_\nu^\dagger \lambda_{N^c})_{IJ} + \frac{v_u}{\sqrt{2}}(A_N)_{IJ}(Y_\nu)_{IJ}.\end{aligned}\quad (13)$$

Using the formula $Z_{\nu IJ}^\dagger \mathcal{M}_{\tilde{n}}^2 Z_{\nu IJ} = \text{diag}(m_{\tilde{\nu}_1}^2, m_{\tilde{\nu}_1}^2, m_{\tilde{\nu}_1}^2, m_{\tilde{\nu}_2}^2, m_{\tilde{\nu}_2}^2, m_{\tilde{\nu}_2}^2)$, the masses of the sneutrinos are obtained.

Because of the introduction of the superfield \hat{N}^c in BLMSSM, the corrected chargino-lepton-sneutrino coupling is adapted as

$$\begin{aligned}\mathcal{L}_{\chi^\pm L \tilde{\nu}} &= - \sum_{I,J=1}^3 \sum_{i,j=1}^2 \bar{\chi}_j^- \left((Y_l)_{IJ} Z_-^{2j*} (Z_{\nu IJ}^\dagger)^{i1} \omega_+ \right. \\ &\quad \left. + \left[\frac{e}{s_W} Z_+^{1j} (Z_{\nu IJ}^\dagger)^{i1} + (Y_\nu)_{IJ} Z_+^{2j} (Z_{\nu IJ}^\dagger)^{i2} \right] \omega_- \right) e^J \tilde{\nu}_i^{I*} + h.c.,\end{aligned}\quad (14)$$

with $\omega_\mp = \frac{1 \mp \gamma_5}{2}$. Here we use the abbreviated form, $s_W = \sin \theta_W$, $c_W = \cos \theta_W$, and θ_W is the Weinberg angle.

From the interactions of gauge and matter multiplets $ig\sqrt{2}T_{ij}^a(\lambda^a \psi_j A_i^* - \bar{\lambda}^a \bar{\psi}_i A_j)$, the lepton-slepton-lepton neutralino couplings are deduced here

$$\mathcal{L}_{l\chi_L^0 \tilde{L}} = \sqrt{2}g_L \bar{\chi}_{L_j}^0 \left(Z_{N_L}^{1j} Z_L^{Ii} \omega_- + Z_{N_L}^{1j*} Z_L^{(I+3)i} \omega_+ \right) l^I \tilde{L}_i^+ + h.c. \quad (15)$$

This type couplings give new contributions beyond MSSM to lepton EDM. Compared with MSSM, there are four new CP violating sources: 1. the mass M_L of gaugino λ_L ; 2. the superfield Higgsino's mass μ_L , which is included in the mass matrices of both sneutrino and lepton neutralino. 3. v_L in Φ_L ; 4. \bar{v}_L in φ_L . In general, we take v_L and \bar{v}_L as real parameters to simplify the numerical discussion.

III. FORMULATION

To obtain the lepton EDM, we use the effective Lagrangian method, and the Feynman amplitudes can be expressed by these dimension-6 operators.

$$\mathcal{O}_1^\mp = \frac{1}{(4\pi)^2} \bar{l}(i\mathcal{D})^3 \omega_\mp l,$$

$$\begin{aligned}
\mathcal{O}_2^\mp &= \frac{eQ_f}{(4\pi)^2} \overline{(i\mathcal{D}_\mu l)} \gamma^\mu F \cdot \sigma \omega_\mp l, \\
\mathcal{O}_3^\mp &= \frac{eQ_f}{(4\pi)^2} \bar{l} F \cdot \sigma \gamma^\mu \omega_\mp (i\mathcal{D}_\mu l), \\
\mathcal{O}_4^\mp &= \frac{eQ_f}{(4\pi)^2} \bar{l} (\partial^\mu F_{\mu\nu}) \gamma^\nu \omega_\mp l, \\
\mathcal{O}_5^\mp &= \frac{m_l}{(4\pi)^2} \bar{l} (i\mathcal{D})^2 \omega_\mp l, \\
\mathcal{O}_6^\mp &= \frac{eQ_f m_l}{(4\pi)^2} \bar{l} F \cdot \sigma \omega_\mp l.
\end{aligned} \tag{16}$$

with $\mathcal{D}_\mu = \partial_\mu + ieA_\mu$, l denoting the lepton fermion, m_l being the lepton mass, $F_{\mu\nu}$ being the electromagnetic field strength. Adopting on-shell condition for external leptons, only $\mathcal{O}_{2,3,6}^\mp$ contribute to lepton EDM. Therefore, the Wilson coefficients of the operators $\mathcal{O}_{2,3,6}^\mp$ in the effective Lagrangian are of interest.

The lepton EDM is expressed as

$$\mathcal{L}_{EDM} = -\frac{i}{2} d_l \bar{l} \sigma^{\mu\nu} \gamma_5 l F_{\mu\nu}. \tag{17}$$

The fermion EDM is a CP violating amplitude which can not be obtained at tree level in the fundamental interactions. However, in the CP violating electroweak theory, one loop diagrams should contribute nonzero value to fermion EDM. Considering the relations between the Wilson coefficients $C_{2,3,6}^\mp$ of the operators $\mathcal{O}_{2,3,6}^\mp$ [13], the lepton EDM is obtained

$$d_l = -\frac{2eQ_f m_l}{(4\pi)^2} \text{Im}(C_2^+ + C_2^{-*} + C_6^+). \tag{18}$$

The one-loop triangle diagrams in BLMSSM are divided into three types according to the virtual particles: 1 the neutralino-slepton diagram; 2 the chargino-sneutrino diagram; 3 the lepton neutralino-slepton diagram. After the calculation, using the on-shell condition for the external leptons, we obtain the one-loop contributions to lepton EDM.

$$\begin{aligned}
d_{li} &= \frac{e}{32\pi^2 \Lambda_{NP}} \text{Im} \left\{ \sum_{i=1}^6 \sum_{j=1}^4 (\mathcal{A}_1)_{ij}^I (\mathcal{A}_2)_{ij}^I \sqrt{x_{\chi_j^0}} \left[\frac{\partial^2}{\partial x_{\tilde{L}_i}^2} \varrho_{2,1}(x_{\chi_j^0}, x_{\tilde{L}_i}) - 2 \frac{\partial}{\partial x_{\tilde{L}_i}} \varrho_{1,1}(x_{\chi_j^0}, x_{\tilde{L}_i}) \right] \right. \\
&+ \sum_{i=1}^6 \sum_{j=1}^3 2g_L^2 (Z_{NL}^{1j*})^2 Z_L^{Ii*} Z_L^{(I+3)i} \sqrt{x_{\chi_{L_j}^0}} \left[\frac{\partial^2}{\partial x_{\tilde{L}_i}^2} \varrho_{2,1}(x_{\chi_{L_j}^0}, x_{\tilde{L}_i}) - 2 \frac{\partial}{\partial x_{\tilde{L}_i}} \varrho_{1,1}(x_{\chi_{L_j}^0}, x_{\tilde{L}_i}) \right] \\
&+ \sum_{J=1}^3 \sum_{i,j=1}^2 (\mathcal{B}_1)_{ij}^{IJ} (\mathcal{B}_2)_{ij}^{IJ} \sqrt{x_{\chi_j^\mp}} \left[\frac{\partial^2}{\partial x_{\tilde{\nu}_i^J}^2} \varrho_{2,1}(x_{\chi_j^\mp}, x_{\tilde{\nu}_i^J}) - 2 \frac{\partial}{\partial x_{\tilde{\nu}_i^J}} \varrho_{1,1}(x_{\chi_j^\mp}, x_{\tilde{\nu}_i^J}) \right. \\
&\left. \left. + 2 \frac{\partial}{\partial x_{\chi_j^\mp}} \varrho_{1,1}(x_{\chi_j^\mp}, x_{\tilde{\nu}_i^J}) \right] \right\},
\end{aligned} \tag{19}$$

with x_i denoting $\frac{m_i^2}{\Lambda_{NP}^2}$, Λ_{NP} representing energy scale of the new physics. The concrete form of the function $\varrho_{i,j}(x, y)$ is shown here

$$\varrho_{i,j}(x, y) = \frac{x^i \ln^j x - y^i \ln^j y}{x - y}. \quad (20)$$

The couplings $(\mathcal{A}_1)_{ij}^I, (\mathcal{A}_2)_{ij}^I, (\mathcal{B}_1)_{ij}^{IJ}$ and $(\mathcal{B}_2)_{ij}^{IJ}$ read as

$$\begin{aligned} (\mathcal{A}_1)_{ij}^I &= \frac{e}{\sqrt{2}s_W c_W} Z_L^{Ii*} (Z_N^{1j*} s_W + Z_N^{2j*} c_W) + (Y_l)_{II}^* Z_{\tilde{L}}^{(I+3)i*} Z_N^{3j*}, \\ (\mathcal{A}_2)_{ij}^I &= -\frac{e\sqrt{2}}{c_W} Z_{\tilde{L}}^{(I+3)i} Z_N^{1j*} + (Y_l)_{II} Z_{\tilde{L}}^{Ii} Z_N^{3j*}, \\ (\mathcal{B}_1)_{ij}^{IJ} &= \frac{e}{s_W} Z_+^{1j*} (Z_{\nu IJ})^{1i} + (Y_\nu)_{IJ}^* Z_+^{2j*} (Z_{\nu IJ})^{2i}, \\ (\mathcal{B}_2)_{ij}^{IJ} &= (Y_l)_{IJ} Z_-^{2j*} (Z_{\nu IJ})^{1i*}. \end{aligned} \quad (21)$$

The matrices $Z_{\tilde{L}}, Z_N$ respectively diagonalize the mass matrices of slepton and neutralino.

To explicit the phase of λ_L obviously in the one loop contributions, we suppose $M_L \gg \mu_L, g_L v_L, g_L \bar{v}_L$. Then the lepton neutralino-slepton contributions are simplified as

$$\begin{aligned} d_l^{\lambda_L \tilde{L}} &= \frac{e}{8\pi^2 \Lambda_{NP}^2} \text{Im} \left\{ \sum_{i=1}^6 g_L^2 Z_L^{Ii*} Z_L^{(I+3)i} |M_L| e^{i\theta_L} \right. \\ &\quad \times \left[\frac{\partial^2}{\partial x_{\tilde{L}_i}^2} \varrho_{2,1} \left(\frac{4|M_L|^2}{\Lambda_{NP}^2}, x_{\tilde{L}_i} \right) - 2 \frac{\partial}{\partial x_{\tilde{L}_i}} \varrho_{1,1} \left(\frac{4|M_L|^2}{\Lambda_{NP}^2}, x_{\tilde{L}_i} \right) \right] \Big\}. \end{aligned} \quad (22)$$

In this formula, the CP violating phase θ_L is conspicuous.

IV. THE NUMERICAL RESULTS

For the numerical discussion, we take into account of the lightest neutral CP-even Higgs mass $m_{h^0} \simeq 125.7$ GeV [15] and the neutrino experiment data[16, 17]

$$\begin{aligned} \sin^2 2\theta_{13} &= 0.090 \pm 0.009, \quad \sin^2 \theta_{12} = 0.306_{-0.015}^{+0.018}, \quad \sin^2 \theta_{23} = 0.42_{-0.03}^{+0.08}, \\ \Delta m_{\odot}^2 &= 7.58_{-0.26}^{+0.22} \times 10^{-5} \text{eV}^2, \quad |\Delta m_A^2| = 2.35_{-0.09}^{+0.12} \times 10^{-3} \text{eV}^2. \end{aligned} \quad (23)$$

In our previous works, the neutron EDM and muon MDM are studied[9, 18], so the constraints from them are also considered here.

We give out the used parameters[18–20]

$$m_e = 0.51 \times 10^{-3} \text{GeV}, \quad m_\mu = 0.105 \text{GeV}, \quad m_\tau = 1.777 \text{GeV},$$

$$\begin{aligned}
m_W &= 80.385\text{GeV}, \quad \alpha(m_Z) = 1/128, \quad s_W^2(m_Z) = 0.23, \\
\tan \beta_L &= 2, \quad L_4 = \frac{3}{2}, \quad m_{Z_L} = 1\text{TeV}, \quad \Lambda_{NP} = 1000\text{GeV}, \\
(Y_\nu)_{11} &= 1.3031 * 10^{-6}, \quad (Y_\nu)_{12} = 9.0884 * 10^{-8}, \quad (Y_\nu)_{13} = 6.9408 * 10^{-8}, \\
(Y_\nu)_{22} &= 1.6002 * 10^{-6}, \quad (Y_\nu)_{23} = 3.4872 * 10^{-7}, \quad (Y_\nu)_{33} = 1.7208 * 10^{-6}, \\
\lambda_{N^c} &= 1, \quad g_L = 1/6, \quad (A_{N^c})_{ii} = (A_N)_{ii} = 3000\text{GeV}, \quad \text{for } i = 1, 2, 3, \\
m_1 &= M1 * e^{i\theta_1}, \quad m_2 = M2 * e^{i\theta_2}, \quad \mu_H = MU * e^{i\theta_\mu}, \quad \sqrt{v_L^2 + \bar{v}_L^2} = v_{L_t}. \quad (24)
\end{aligned}$$

Here, θ_1, θ_2 and θ_μ are the CP violating phases of the parameters m_1, m_2 , and μ_H . We consider two new CP violating parameters with the phases θ_{μ_L} and θ_L

$$\mu_L = muL * e^{i\theta_{\mu_L}}, \quad M_L = ML * e^{i\theta_L}. \quad (25)$$

To simplify the numerical discussion, we use the following relations.

$$\begin{aligned}
(m_L^2)_{11} &= (m_L^2)_{22} = (m_L^2)_{33} = S_L, \quad (m_R^2)_{11} = (m_R^2)_{22} = (m_R^2)_{33} = S_R, \\
(m_{N^c}^2)_{11} &= (m_{N^c}^2)_{22} = (m_{N^c}^2)_{33} = S_\nu, \quad (A_l)_{11} = (A_l)_{22} = (A_l)_{33} = AL. \quad (26)
\end{aligned}$$

If we do not specially declare, the non-diagonal elements of the used parameters should be zero.

To study the effects to lepton EDM from the non-diagonal elements of the used parameters, we consider the constraints from the lepton flavor violating processes $l_j \rightarrow l_i + \gamma$ and $l_j \rightarrow 3l_i$. The experiment upper bounds of $Br(\mu \rightarrow e + \gamma)$ and $Br(\mu \rightarrow 3e)$ are respectively 5.7×10^{-13} and 1.0×10^{-12} . They are both strict and set severe limits on the parameter space, especially for the sensitive parameters including non-diagonal elements for the lepton flavor violation. In our prepared work[21], we study $Br(\mu \rightarrow e + \gamma)$ and $Br(\mu \rightarrow 3e)$, and find that the virtual particle masses, $\tan \beta$ and the ratios of non-diagonal elements to diagonal elements for the slepton(sneutrino) mass squared matrices are important parameters. When the slepton and sneutrino are at TeV order, $\tan \beta$ should be in the region $10 \sim 20$. The effects to $\mu \rightarrow e + \gamma$ and $\mu \rightarrow 3e$ from the non-diagonal elements of $m_{N^c}^2, A_{N^c}$ and A_N are not large. On the other hand, the non-diagonal elements of m_L^2, m_R^2 influence the both LFV processes strong. With the supposition $(m_L^2)_{ij} = (m_R^2)_{ij} = FL^2$, FL should be in the range $(0 \sim 500)\text{GeV}$ except extreme parameter space.

A. the electron EDM

At first, we study electron EDM, because its upper bound is the most strict one. The CP violating phases $\theta_1, \theta_2, \theta_\mu, \theta_{\mu_L}, \theta_L$, and other parameters have close relationships with electron EDM. In this subsection, we suppose $S_\nu = 1.0 \times 10^6 \text{GeV}^2, m_L = 1000 \text{GeV}$ and $v_{L_t} = 3000 \text{GeV}$.

Supposing $\theta_1 = \theta_2 = \theta_\mu = \theta_L = 0$, we study the contributions from θ_{μ_L} to electron EDM. μ_L relates with sneutrino mass squared matrix and lepton neutralino mass matrix. Here, the contributions to lepton EDM from the lepton neutralino-slepton diagram are dominant, because the chargino-sneutrino diagram contributions are suppressed by the tiny neutrino Yukawa couplings through $\text{Im}[(Y_\nu)_{IJ}^*(Z_{\nu IJ})^{2i}(Z_{\nu IJ})^{1i*}]$. With $\theta_{\mu_L} = 0.5\pi, \tan\beta = 15, \mu_H = -800 \text{GeV}, m_2 = 800 \text{GeV}, m_1 = 1000 \text{GeV}$, in Fig.(1) we plot the solid line, dotted line and dashed line versus muL ($-2000 \sim 2000 \text{ GeV}$) corresponding to $S_R = S_L = (6 \times 10^6, 8 \times 10^6, 10 \times 10^6) \text{GeV}^2$. When $|muL|$ is around 1000GeV , $|d_e|$ reaches its biggest value. For the same positive muL , the solid line is up the dotted line and the dotted line is up the dashed line. It implies that heavier slepton masses lead to smaller lepton neutralino-slepton contributions. The largest values of the three lines are respectively $1.4 \times 10^{-28} e.cm, 0.8 \times 10^{-28} e.cm$ and $0.4 \times 10^{-28} e.cm$. As $|muL| > 1000 \text{GeV}$, $|d_e|$ is the decreasing function of $|muL|$, which is reasonable because large muL should suppress the results.

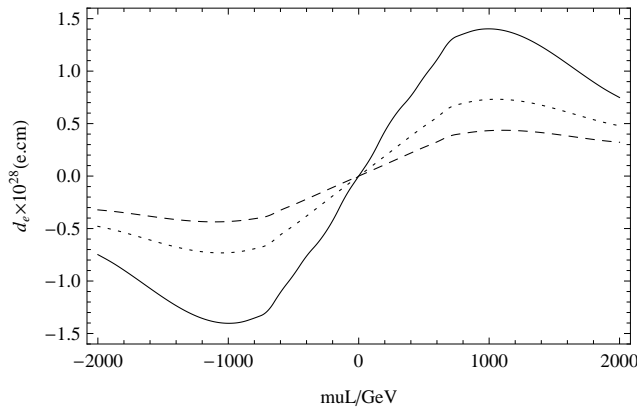


FIG. 1: With $\theta_{\mu_L} = 0.5\pi$ and $\theta_1 = \theta_2 = \theta_\mu = \theta_L = 0$, the contributions to electron EDM varying with muL are plotted by the solid line, dotted line and dashed line respectively corresponding to $S_R = S_L = (6 \times 10^6, 8 \times 10^6, 10 \times 10^6) \text{GeV}^2$.

In the follow of this subsection, the parameters $S_L = 6.0 \times 10^6 \text{GeV}^2, S_R = 1.0 \times$

10^6GeV^2 , $\mu_L = -3000 \text{GeV}$ are adopted. The mass squared matrix of slepton has the parameter AL leading to the influence of electron EDM. With the parameters $m_1 = 1000 \text{GeV}$, $m_2 = 600 \text{GeV}$, $MU = -800 \text{GeV}$, $\theta_\mu = 0.5\pi$, $(A'_l)_{11} = (A'_l)_{22} = (A'_l)_{33} = 200 \text{GeV}$ and $\tan \beta = (10, 15, 25)$, the results are shown by the solid line, dotted line and dashed line respectively in Fig.(2). These three lines are all decreasing functions of AL in the region $(-3000 \sim 3000) \text{GeV}$, and their values vary in the range $(1.8 \sim 6.6) \times 10^{-29} e.cm$. Generally speaking, larger $\tan \beta$ leads to larger d_e . The contributions from the right-handed sneutrino have nothing to do with AL . For the dashed line, the right-handed sneutrino contributions are about $1.4 \times 10^{-29} e.cm$; For the dotted line, the right-handed sneutrino corrections are around $1.0 \times 10^{-29} e.cm$; For the solid line, the right-handed sneutrino contributions are about $0.7 \times 10^{-29} e.cm$. The lepton neutralino-slepton diagram also gives important contributions and they vary from $0.5 \times 10^{-29} e.cm$ to $1.5 \times 10^{-29} e.cm$ for the three lines. It is obviously that the contributions from the right-handed sneutrino and lepton neutralino are very important.

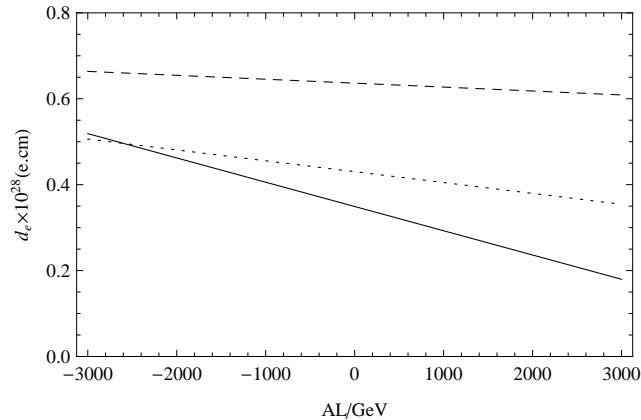


FIG. 2: With $\theta_\mu = 0.5\pi$, $\theta_1 = \theta_2 = \theta_{\mu_L} = \theta_L = 0$ and $\tan \beta = (10, 15, 25)$, the contributions to electron EDM varying with AL are plotted by the solid line, dotted line and dashed line respectively.

m_1 relates with the neutralino mass matrix. So we study the numerical results versus $M1$ with $\theta_1 = 0.5\pi$, $m_2 = 750 \text{GeV}$, $(A'_l)_{11} = -135 \text{GeV}$, $(A'_l)_{22} = (A'_l)_{33} = 200 \text{GeV}$, $\tan \beta = 15$, $AL = -2000 \text{GeV}$, $\mu_H = (-500, -1000, -2000) \text{GeV}$, and the corresponding results are plotted by the solid line, dotted line and dashed line in Fig.(3). The three lines are very similar. The biggest value is about $12 \times 10^{-29} e.cm$, as $M1 = -600 \text{GeV}$. The absolute value of d_e turns small slowly with the enlarging $|M1|$ in the region $(600 \sim 3000) \text{GeV}$. When $|M1|$

is biggish, the masses of neutralinos are heavy, which suppresses the contributions to electron EDM. At the point $M1 = 0$, there is none CP violating effect and $d_e = 0$ is reasonable. The right-handed sneutrino contributions are related with θ_2 and θ_μ through the coupling with chargino. The lepton neutralino-slepton contributions have relations with $\theta_\mu, \theta_{\mu_L}, \theta_L$. In this condition, only θ_1 is nonzero, then both the right-handed sneutrino and lepton neutralino give none contribution to d_e .

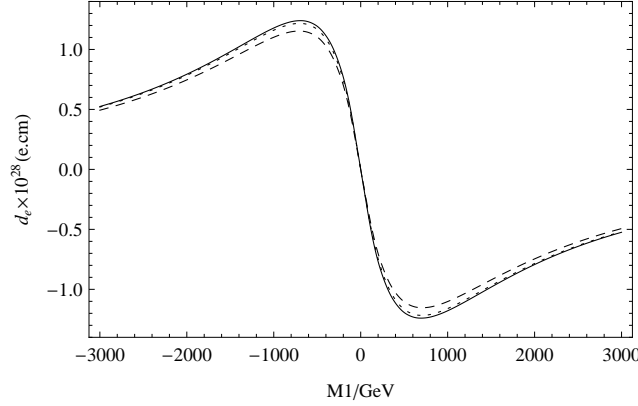


FIG. 3: With $\theta_1 = 0.5\pi, \theta_2 = \theta_\mu = \theta_{\mu_L} = \theta_L = 0$ and $\mu_H = (-500, -1000, -2000)\text{GeV}$, the contributions to electron EDM varying with $M1$ are plotted by the solid line, dotted line and dashed line respectively.

m_2 is included in the mass matrices of neutralino and chargino, so θ_2 is very important for electron EDM. As $\theta_2 = 0.5\pi$, we study the effects from some non-diagonal elements of $m_{\tilde{N}_c}^2$. With the parameters $m_1 = 1000\text{GeV}, \mu_H = -800\text{GeV}, (A'_l)_{11} = (A'_l)_{22} = (A'_l)_{33} = 200\text{GeV}, \tan\beta = 15, AL = -2000\text{GeV}$, we adopt $(m_{\tilde{N}_c}^2)_{12} = (m_{\tilde{N}_c}^2)_{21} = MF^2$, and the other non-diagonal elements of $m_{\tilde{N}_c}^2$ are zero. For $M2 = (700, 1000)\text{GeV}$, the total one loop results are represented by the dashed line and dotted line respectively in the Fig.(4). At the same time, in Fig.(4) the contributions from the right-handed sneutrino are also plotted by the solid line and dot-dashed line corresponding to $M2 = (700, 1000)\text{GeV}$. The dashed line and dotted line are in the region $(8.5 \sim 9.3) \times 10^{-29} e.cm$ and they are both very slowly increasing functions of MF . The solid line and dot-dashed line increase quickly, when MF turns from 0 to 60 GeV. In the MF region $(60 \sim 1000)\text{GeV}$, the solid line and dot-dashed line turn large slowly. As $MF = 0$, the right-handed sneutrino corrections are around $1.0 \times 10^{-29} e.cm$. When MF is larger than 60 GeV, the contributions from the right-handed sneutrino can reach $2.0 \times 10^{-29} e.cm$. Therefore, they are important and decrease the effects from the left-

handed sneutrino to some extent with nonzero MF . Because of $\theta_\mu = \theta_{\mu_L} = \theta_L = 0$, lepton neutralino-slepton diagram does not give corrections to electron EDM in this condition. From the Figs.(1, 2, 3, 4), one can find the upper bound of electron EDM is strict and has rigorous bound on the parameter space.

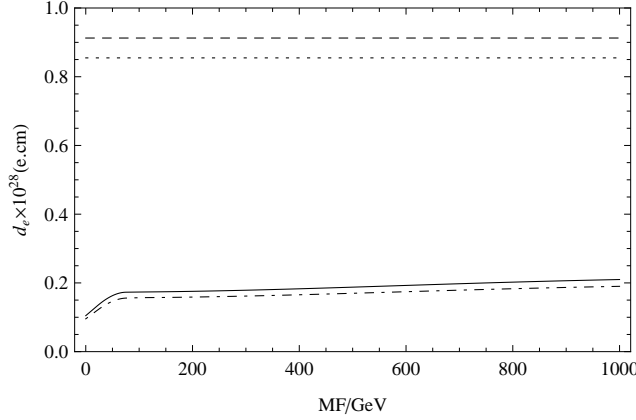


FIG. 4: With $\theta_2 = 0.5\pi, \theta_1 = \theta_\mu = \theta_{\mu_L} = \theta_L = 0$ and $M2 = (700, 1000)\text{GeV}$, the contributions to electron EDM varying with MF are plotted by the dashed line and dotted line respectively; the right-handed sneutrino contributions are plotted by the solid line and dot-dashed line respectively.

B. the muon EDM

Lepton EDM is CP violating which is generated by the CP violating phases. In the similar way, the muon EDM is numerically studied. The parameters $S_L = 7.0 \times 10^6 \text{GeV}^2, S_R = 6.0 \times 10^6 \text{GeV}^2, S_\nu = 2.0 \times 10^6 \text{GeV}^2, AL = -1000 \text{GeV}, \mu_L = -3000 \text{GeV}, ML = 2000 \text{GeV}, (A'_l)_{11} = (A'_l)_{22} = (A'_l)_{33} = 200 \text{GeV}$ are supposed here.

The lepton neutrino mass matrix includes the new CP violating phase θ_L . Therefore, it obviously produces new contributions to the lepton EDM. As $\theta_1 = \theta_2 = \theta_\mu = \theta_{\mu_L} = 0, m_1 = 700 \text{GeV}, m_2 = 800 \text{GeV}, \mu_H = -600 \text{GeV}, \tan \beta = 15$, in Fig.(5) we study d_μ versus θ_L with $v_{L_t} = (1, 3, 5) \text{TeV}$, and the results are plotted by the solid line, dotted line and dashed line. The three lines are of the same shape, and all look like $-\sin \theta_L$. These lines are almost coincident, whose largest values are about $1.9 \times 10^{-26} (e.cm)$. The Fig.(5) implies the effects from v_{L_t} to muon EDM are small. These contributions are only come from lepton neutralino-slepton diagram. The chargino-sneutrino and neutralino-slepton diagrams give zero contribution to d_μ .

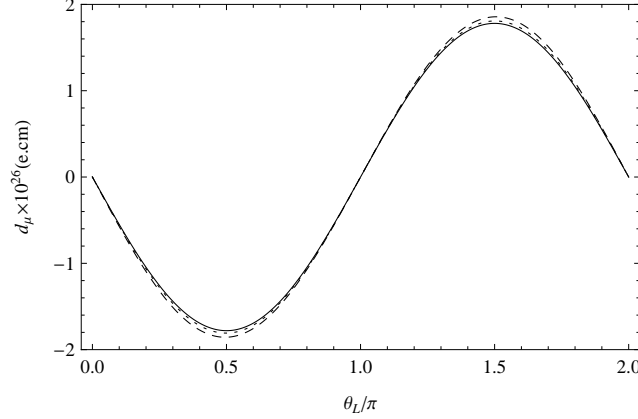


FIG. 5: With $\theta_1 = \theta_2 = \theta_\mu = \theta_{\mu_L} = 0$ and $v_{L_t} = (1, 3, 5)\text{TeV}$, the contributions to muon EDM varying with θ_L are plotted by the solid line, dotted line and dashed line respectively.

As noted in the front subsection, m_2 is an important parameter for the lepton EDM. Using $m_1 = 700\text{GeV}$, $\theta_2 = 0.5\pi$, $\mu_H = -600\text{GeV}$, $v_{L_t} = 3000\text{GeV}$, $\tan\beta = (15, 25, 35)$, we study d_μ versus $M2$ in Fig.(6), and the numerical results are plotted by the solid line, dotted line and dashed line respectively. At the point $M2 = \pm 400\text{ GeV}$, the absolute value of each line reaches its biggest value. The dashed line can arrive at $2.0 \times 10^{-26}e.cm$. Larger $|M2|$ leads to smaller d_μ for the three lines, when $|M2|$ is larger than 400GeV . As $|M2|$ is very big, heavy neutralinos and charginos are produced, which suppresses the contributions to muon EDM. The order from big to small for the absolute values of the three lines is the dashed line $>$ the dotted line $>$ the solid line. The corrections from the right-handed sneutrino are about $(23 \sim 25)\%$ of d_μ . As $\theta_\mu = \theta_{\mu_L} = \theta_L = 0$, lepton neutralino-slepton contributions are zero.

m_L^2 and m_R^2 influence the masses of slepton and sneutrino. The non-diagonal elements of m_L^2 and m_R^2 may give considerable contributions. To simplify the discussion, we suppose the relations $(m_L^2)_{ij} = (m_R^2)_{ij} = FL^2$, for $(i \neq j; i, j = 1, 2, 3)$ and adopt the parameters $m_1 = 1000\text{GeV}$, $M2 = 750\text{GeV}$, $v_{L_t} = 3000\text{GeV}$, $\theta_2 = 0.5\pi$, $\tan\beta = 15$. In Fig.(7), the solid line, dotted line and dashed line, respectively represent the results with $\mu_H = (-500, -700, -1500)\text{GeV}$. They are all increasing functions of FL , and the solid line is the highest line. The dotted line is the middle one. These numerical results are in the range $0.6 \sim 1.2 \times 10^{-26}e.cm$. When FL varies from 0 to 50GeV , though the total results do not have significant change, the contributions of the right-handed sneutrino increase quickly.

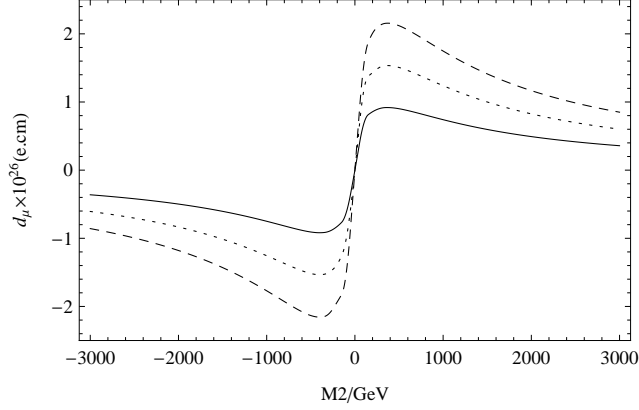


FIG. 6: With $\theta_2 = 0.5\pi, \theta_1 = \theta_\mu = \theta_{\mu_L} = \theta_L = 0$ and $\tan\beta = (15, 25, 35)$, the contributions to muon EDM varying with $M2$ are plotted by the solid line, dotted line and dashed line respectively.

The reason is that left-handed sneutrino corrections turn small fast with the non-diagonal elements of m_L^2 and m_R^2 . Right-handed sneutrino and left-handed sneutrino mix and should be regarded as an entirety. To some extent, non-zero FL moves the contributions from left-handed sneutrino to the right-handed sneutrino, without affecting the total results obviously. The ratios for the right-handed sneutrino contributions to d_μ ran from 20% to bigger values, and can even reach 50%. With our used parameters, the numerical results for muon EDM shown as the Figs. (5,6,7) are about at the order of $10^{-26}e.cm$, which is almost seven-order smaller than muon EDM upper bound.

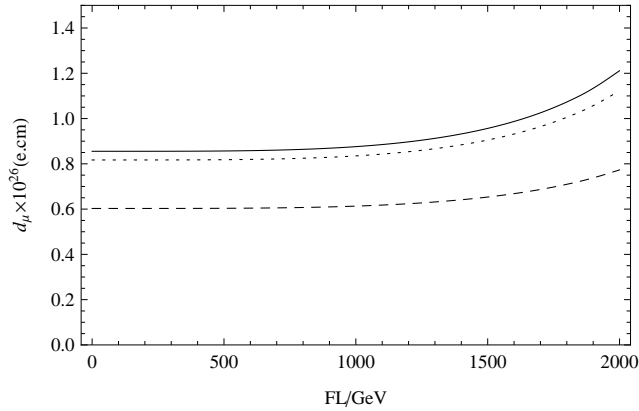


FIG. 7: With $\theta_2 = 0.5\pi, \theta_1 = \theta_\mu = \theta_{\mu_L} = \theta_L = 0$ and $MU = (-500, -700, -1500)\text{GeV}$, the contributions to muon EDM varying with FL are plotted by the solid line, dotted line and dashed line respectively.

C. the tau EDM

Tau is the heaviest lepton, whose EDM upper bound is the largest one and at the order of $10^{-17}e.cm$. Tau EDM is also of interest and calculated here. In this subsection, we use $S_\nu = 2.0 \times 10^6 \text{GeV}^2$, $AL = -1000 \text{GeV}$, $(A'_l)_{11} = (A'_l)_{22} = (A'_l)_{33} = 200 \text{GeV}$, $m_1 = 1000 \text{GeV}$, $\mu_L = -3000 \text{GeV}$, $ML = 3000 \text{GeV}$, $v_{L_t} = 3000 \text{GeV}$.

With $\theta_1 = \theta_2 = \theta_\mu = \theta_{\mu_L} = 0$, $\tan \beta = 15$, $m_2 = 800 \text{GeV}$, $\mu_H = -800 \text{GeV}$ and supposing $S_L = S_R = s_m^2$, we plot the results versus s_m by the solid line, dotted line and dashed line for $\theta_L = (-0.1, -0.3, -0.5)\pi$. Under this supposition, only lepton neutralino-slepton diagram gives nonzero corrections. In Fig.(8), one can find d_τ is the decreasing function of s_m . In the s_m region $(600 \sim 1000) \text{GeV}$, the three lines decrease quickly with the enlarging s_m . As $s_m = 600 \text{GeV}$, the dashed line can reach $4 \times 10^{-24} e.cm$ and even larger. When $s_m > 1000 \text{GeV}$, the results decrease slowly and are almost coincident as $s_m > 2000 \text{GeV}$. At the points $s_m = (1000, 2000) \text{GeV}$, the results are at the order of $(10^{-25}, 10^{-26}) e.cm$.

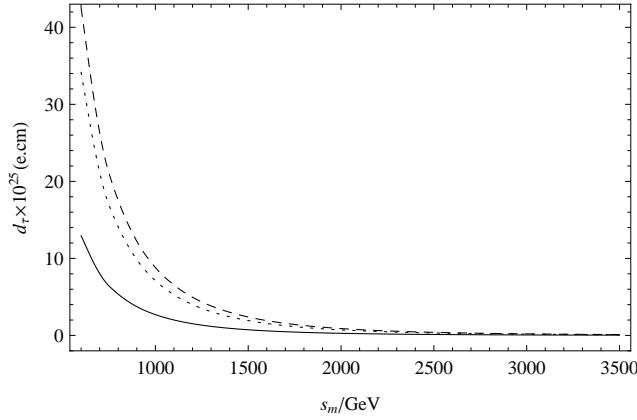


FIG. 8: With $\theta_1 = \theta_2 = \theta_\mu = \theta_{\mu_L} = 0$ and $\theta_L = (-0.1, -0.3, -0.5)\pi$, the contributions to tau EDM varying with s_m are plotted by the solid line, dotted line and dashed line respectively.

The relation between d_τ and μ_H is studied here. We use the parameters $S_L = 7.0 \times 10^6 \text{GeV}^2$, $S_R = 6.0 \times 10^6 \text{GeV}^2$, $m_2 = 750 \text{GeV}$, $\theta_\mu = 0.5\pi$, $\tan\beta = (10, 15, 25)$, and plot the results by the solid line, dotted line and dashed line respectively in the Fig.(9). The dashed line reaches $2.4 \times 10^{-25} e.cm$ as $MU = -500 \text{GeV}$. When $|MU| > 500 \text{GeV}$, the abstract values of the numerical results shrink with the enlarging $|MU|$. Larger $\tan\beta$ results in larger d_τ , when the other parameters are same. The right-handed sneutrino contributions are about $(15 \sim 20)\%$ of the total results for the three lines. At the same time, the lepton neutralino-slepton contributions can match the right-handed sneutrino contributions, and they are at the same order.

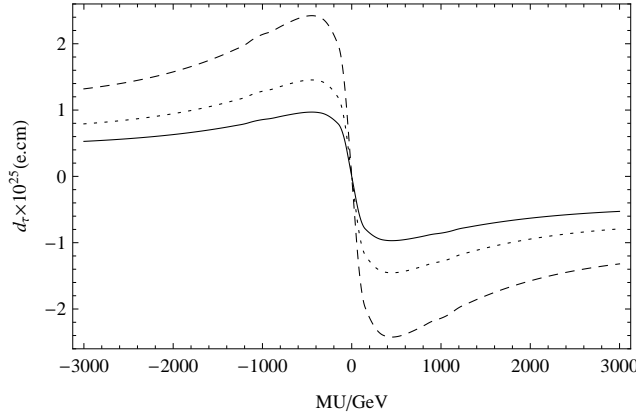


FIG. 9: With $\theta_\mu = 0.5\pi$, $\theta_1 = \theta_2 = \theta_{\mu_L} = \theta_L = 0$ and $\tan\beta = (10, 15, 25)$, the contributions to tau EDM varying with MU are plotted by the solid line, dotted line and dashed line respectively.

The parameters in BLMSSM and absent in MSSM should affect d_τ to some extent. With the parameters $S_L = 7.0 \times 10^6 \text{GeV}^2$, $S_R = 6.0 \times 10^6 \text{GeV}^2$, $\theta_2 = 0.5\pi$, $\mu_H = -800 \text{GeV}$, $\tan\beta = 15$ and based on the assumption $(A_{N^c})_{ij} = (A_N)_{ij} = NF$, for $i \neq j$ and $i, j = 1, 2, 3$, we research the effects from the non-diagonal elements of A_{N^c} and A_N . In Fig.(10), the solid line, dotted line and dashed line correspond respectively to the results obtained with $M2 = (500, 1000, 1500) \text{GeV}$. When NF is near 2000GeV , the results increase observably. The solid line is up the dotted line, and the dotted line is up the dashed line. The values of the three lines are in the region $(1.0 \sim 1.5) \times 10^{-25} e.cm$. The right-handed sneutrino contributions largen quickly with the increasing $|NF|$, and their ratios to the total results improve from 24% to 50%. The reason should be that the non-diagonal elements of A_{N^c} and A_N weaken the left-handed sneutrino contributions. At the same time the contributions from the right-hand sneutrino are enhanced. Generally speaking, in BLMSSM the left-and right-

handed sneutrinos are an integral whole, and should be discussed together. The Figs.(8,9,10) show that the one-loop contributions to tau EDM are at the order of $10^{-25} \sim 10^{-24}(e.cm)$ in our used parameter space. These contributions are about eight-order smaller than the upper bound of tau EDM.

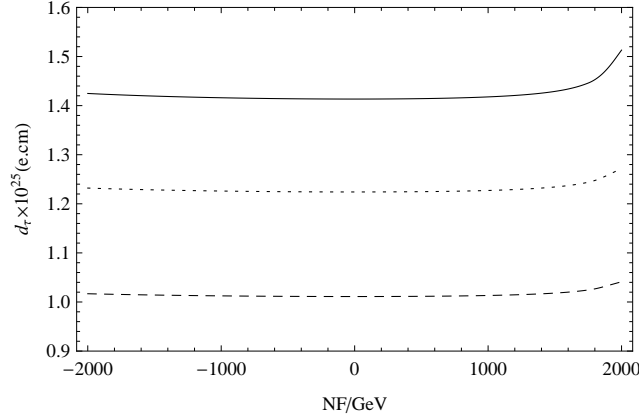


FIG. 10: With $\theta_2 = 0.5\pi, \theta_1 = \theta_\mu = \theta_{\mu_L} = \theta_L = 0$ and $M_2 = (500, 1000, 1500)\text{GeV}$, the contributions to tau EDM varying with NF are plotted by the solid line, dotted line and dashed line respectively.

V. DISCUSSION AND CONCLUSION

In the frame work of CP violating BLMSSM, we study the one-loop contributions to the lepton(e, μ, τ) EDM. The used parameters can satisfy the experiment data of Higgs and neutrino. The effects of the CP violating phases $\theta_1, \theta_2, \theta_\mu, \theta_{\mu_L}, \theta_L$ to the lepton EDM are researched. The upper bound of electron EDM is $8.7 \times 10^{-29}e.cm$, which gives strict confine on the BLMSSM parameter space. In our used parameter space, the contributions to electron EDM can easily reach its upper bound and even exceed it. The numerical values obtained for muon EDM and tau EDM are at the order of $10^{-26}e.cm$ and $10^{-25} \sim 10^{-24}e.cm$ respectively. They both are several-order smaller than their EDM upper bounds. Our numerical results mainly obey the rule $d_e/d_\mu/d_\tau \sim m_e/m_\mu/m_\tau$. The right-handed sneutrino contributions are considerable, and should be taken into account. The contributions from the lepton neutralino-slepton have two new CP violating sources, and include the coupling constant g_L . If we enlarge g_L and adopt other parameters, the lepton neutralino-slepton

contributions to lepton EDM can enhance several orders. In general, the numerical results of the lepton EDM are large, and they maybe detected by the experiments in the near future.

Acknowledgements

This work has been supported by the National Natural Science Foundation of China (NNSFC) with Grants No. (11275036, 11447111), the open project of State Key Laboratory of Mathematics-Mechanization with Grant No. Y5KF131CJ1, the Natural Science Foundation of Hebei province with Grant No. A2013201277, and the Found of Hebei province with the Grant NO. BR2-201 and the Natural Science Fund of Hebei University with Grants No. 2011JQ05 and No. 2012-242, Hebei Key Lab of Optic-Electronic Information and Materials, the midwest universities comprehensive strength promotion project.

-
- [1] M.E. Pospelov and I.B. Khriplovich, Sov. J. Nucl. Phys. **53** (1991) 638; Yad. Fiz. 53 (1991) 1030; M. Pospelov and A. Ritz, Phys. Rev. D **89** (2014) 056006.
 - [2] J. Baron et al. [ACME Collaboration], Science V. **343**, N. 6168 (2014) 269; arXiv:1310.7534.
 - [3] J. Beringer et al. (Particle Data Group), Phys. Rev. D **86** (2012) 010001; T. Ibrahim, A. Itani, P. Nath, arXiv:1406.0083; M. Jung, arXiv:1405.6389.
 - [4] J. Rosiek, Phys.Rev. D **41** (1990) 3464; arXiv:hep-ph/9511250; Tai-Fu Feng, Xiu-Yi Yang, Nucl.Phys. B **814** (2009) 101; H.P. Nilles, Phys. Rept. **110** (1984) 1; H.E. Haber and G.L. Kane, Phys. Rept. **117** (1985) 75;
 - [5] T. Ibrahim and P. Nath, Phys. Rev. D **57** (1998) 478; Phys. Rev. D **58**(1998) 019901; Phys. Rev. D **58** (1998) 111301; Phys. Rev. D **60**(1999) 099902.
 - [6] P. F. Perez, Phys. Lett. B **711** (2012) 353; J. M. Arnold, P. F. Perez, B. Fornal, and S. Spinner, Phys. Rev. D **85** (2012)115024.
 - [7] P. F. Perez and M. B. Wise, JHEP **1108** (2011) 068; Phys. Rev. D **82** (2010) 011901;
 - [8] Tai-Fu Feng, Shu-Min Zhao, Hai-Bin Zhang, et al., Nucl. Phys. B **871** (2013) 223.
 - [9] Shu-Min Zhao, Tai-Fu Feng, Ben Yan et al., JHEP **1310** (2013) 020.
 - [10] Fei Sun, Tai-Fu Feng, Shu-Min Zhao et al., Nucl.Phys. B **888** (2014) 30.
 - [11] S. Heinemeyer, D. Stockinger and G. Weiglein, Nucl. Phys. B **699** (2004) 103 ; T.F. Feng, T. Huang, X.Q. Li, X.M. Zhang and S.M. Zhao, Phys. Rev. D **68** (2003) 016004; X.Y. Yang and

- T.F. Feng, Phys. Lett. B **675** (2009) 43.
- [12] T. Abe, J. Hisano, T. Kitahara, K. Tobioka, JHEP **1401** (2014) 106; S. Ipek, Phys. Rev. D **89** (2014) 073012.
 - [13] A. Pilaftsis, Phys. Rev. D **58** (1998) 096010; M. Carena, J. Ellis, A. Pilaftsis et al., Nucl. Phys. B **586** (2000) 92; Tai-Fu Feng, Lin Sun, Xiu-Yi Yang, Nucl. Phys. B **800** (2008) 221; N. Yamanaka, Phys. Rev. D **87**, (2013)011701.
 - [14] X.G. He, C.J. Lee, S.F. Li, J. Tandean, JHEP **1408** (2014) 019; X.G. He, C.J. Lee, S.F. Li, J. Tandean, Phys. Rev. D **89** (2014) 091901.
 - [15] CMS Collaboration, Phys. Lett. B **716** (2012) 30; ATLAS Collaboration, Phys. Lett. B **716** (2012) 1; CMS Collaboration arXiv:hep-ph/1301.3405.
 - [16] K. Abe et al.(T2K Collaboration), Phys. Rev. Lett. **107** (2011) 041801; F.An et al. (DAYA-BAY Collaboration), Phys. Rev. Lett. **108** (2012) 171803; J. Ahn et al. (RENO Collaboration), Phys. Rev. Lett. **108** (2012) 191802.
 - [17] M. Gonzalez-Garcia, M. Maltoni, J. Salvado, and T. Schwetz, J. High Energy Phys. **12** (2012) 123; D. V. Forero, M. Trtola, and J.W. F. Valle, Phys. Rev. D **86** (2012) 073012.
 - [18] Shu-Min Zhao, Tai-Fu Feng, Hai-Bin Zhang et al., JHEP **1411** (2014) 119.
 - [19] K.A. Olive et al. (Particle Data Group), Chin. Phys. C **38** (2014) 090001.
 - [20] Chen Biao, Zhao Shu-min, Yan Ben, et al., Commun. Theor. Phys. **61** (2014) 619-623.
 - [21] Shu-Min Zhao, Tai-Fu Feng, Xi-Jie Zhan, et al., Lepton-flavor violation in the BLMSSM, in preparation.